Available online at www.sciencedirect.com

SCIENCE DIRECT®

Solid State Communications 129 (2004) 469–473

solid state communications

www.elsevier.com/locate/ssc

Energy transfer from organic surface adsorbate-polyvinyl pyrrolidone molecules to luminescent centers in ZnS nanocrystals

K. Manzoor[a], S.R. Vadera[a], N. Kumar[a,*], T.R.N. Kutty[b]

[a]*Defence Laboratory, Jodhpur 342 011, India*

[b]*Material Research Center, Indian Institute of Science, Bangalore 560 012, India*

Received 20 August 2003; received in revised form 22 October 2003; accepted 7 November 2003 by A.K. Sood

Abstract

Multi-colour emitting doped ZnS nanocrystals surface capped with pyridine (P-ZnS) or polyvinyl pyrrolidone (PVP-ZnS) have been synthesized by wet chemical methods. The photoluminescence studies show that the dopant related emission from P-ZnS nanocrystals are caused by the energy transfer from band-to-band excitation of the host lattice. However, in the case of PVP capped ZnS, considerable enhancement in the emission intensity was observed and the corresponding excitation spectra appeared dramatically broadened due to the presence of multiple excitation bands with peak maxima at 235, 253, 260, 275, and 310 nm. The bands from 235 to 275 nm are assigned to the electronic transitions in the chemisorbed PVP molecules whereas the excitation maximum around 310 nm corresponds to the band-to-band transition within the nanocrystalline ZnS host. The presence of PVP related energy bands in the excitation spectrum indicates the process of energy transfer from the surface adsorbed PVP molecules to dopant centers in ZnS nanocrystals. This study brings out a heterogeneous sensitizer-activator relation between organic surface adsorbate and doped semiconducting nanocrystals.

PACS: 78.55.m; 78.67.bf

Keywords: A. Nanostructures; D. Electronic band structures; E. Luminescence

1. Introduction

Nanocrystals based on II–VI semiconductors and their doped systems have acquired considerable importance because of their great potential for many versatile applications ranging from DNA markers to light emitting displays [1–4]. Due to large surface to volume ratio of nanoparticles, the atoms situated near the surface regions play a major role in its electronic, optical and thermodynamic properties [5]. At the surface, since the co-ordination number around the atoms is less than that inside the bulk, there can be larger number of defect states which acts as non-radiative pathways for the excited electrons and become detrimental to the luminescent properties of nanocrystalline phosphors [6]. Therefore, it is necessary to modify the nanoparticle surface by using suitable capping agents so that the surface caps will passivate the defect states and dangling bond density.

There are a number of reports on different methods and materials used for the surface capping of nanoparticles [7]. Covering the nanocrystal core surface with an inorganic shell or organic ligand molecules can bring about necessary passivation of vacancies, stabilization of the colloidal suspension and also maintain the quantum confinement effects by way of particle isolation. The adsorbed monolayer also impart structural environment for the attachment of functional molecular entities leading to the fabrication of organic-quantum dot electronic or electro-optic devices [8]. However, till now, there observed no direct involvement of the capping molecules in the luminescence processes of doped semiconducting nanocrystals. In this communication, we report the process of energy transfer from the organic

* Corresponding author. Tel.: +91-291-2514300; fax: +91-291-2511191.

E-mail address: nkjain_jd@yahoo.com (N. Kumar).

0038-1098/$ - see front matter © 2003 Elsevier Ltd. All rights reserved.
doi:10.1016/j.ssc.2003.11.012

surface adsorbate, polyvinyl pyrrolidone, to the dopant ions (Cu^{+}, Cu^{+}–Al^{3+}, or Mn^{2+}) in ZnS nanocrystals resulting in efficient blue, green and orange–red emissions.

2. Experimental

ZnS nanocrystals doped with Cu^{+}, Cu^{+}–Al^{3+} or Mn^{2+} have been synthesized by wet chemical colloidal precipitation method [9]. The synthesis employed co-precipitation reaction of inorganic precursors of Zn^{2+} and S^{2-} with dopant ions (Cu^{+}, Al^{3+} or Mn^{2+}) in an aqueous medium containing the capping molecules. The dopant concentrations and stoichiometric condition, $X = [S^{2-}]/[Zn^{2+}]$ ratio, have been optimized in order to obtain saturated emission colours in blue, green and orange–red. Various surface capping agents such as pyridine (P), acrylic acid (Aa), methacrylic acid (MAa), mercapto acetic acid, poly acrylic acid (PAa), polyvinyl alcohol (PVA) and polyvinyl pyrrolidone (PVP) have been used for the surface modification of nanocrystals. Among these, the PVP-capped nanoparticles (PVP-ZnS) showed remarkably high emission intensity compared to the nanoparticles capped with any other agent. To evaluate the enhanced emission characteristics due to PVP capping, detailed studies have been carried out on different PVP-ZnS doped systems and the results are compared with that of pyridine capped nanoparticles (P-ZnS). The crystallinity of the samples have been studied by using X-ray diffractometer, Philips XRG-3000 fitted with a Cu K_{α} ($\lambda = 1.54056$ nm) source. The size and shape of the nanoparticles were studied by using transmission electron microscope (TEM), JEOL-JEM-200CX. Atomic absorption spectrophotometer (AAS, Perkin–Elmer-2380) has been used to estimate the doping concentrations of Cu^{+}, Al^{3+} and Mn^{2+} in ZnS nanocrystals. Photoluminescence emission (PL) and excitation (PLE) studies, at room temperature, have been carried out by using Spectrofluorometer, JASCO-FP-6500 fitted with a 350W Xenon flash lamp and R-928 PMT detector.

3. Results and discussions

Fig. 1(a) shows the XRD pattern of ZnS nanoparticles, indicating the zinc-blende (cubic, β-ZnS) structure. The broad diffraction peaks are attributed to the characteristic small particle effect [10]. It was found that the changes in surface capping molecule do not have any effect in the crystal structure of nanoparticles. TEM image of PVP-ZnS and P-ZnS particles, shown in Fig. 1(b), indicate the formation of well isolated particles of average size ~4 nm in both the cases. Further, it is found that the PVP capped particles have better monodispersity than the Pyridine capped particles.

Fig. 2 shows the PL spectra of ZnS: 0.13% Cu^{+} (S_B),

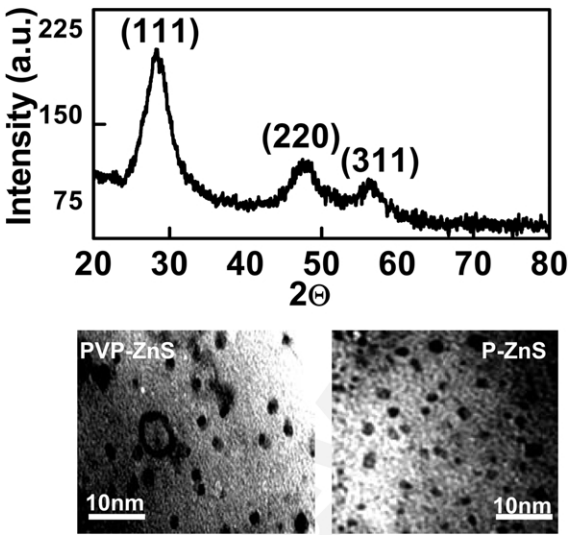

Fig. 1. XRD pattern and bright field TEM images of doped ZnS nanoparticles.

ZnS: 0.13% Cu^{+}, 0.1% Al^{3+} (S_G) and ZnS: 0.2% Mn^{2+} (S_O) samples emitting in blue (472 nm), green (530 nm) and orange–red (590 nm) colours, respectively. It was found that the emission characteristics of ZnS nanoparticles depend not only on the dopant ions but also on the concentration of vacancy centers [9]. The blue emission from the sample S_B has been found most efficient when the nanoparticles are prepared under off-stoichiometric condition of $X < 1$. It was reported that the samples prepared under sulphur deficient condition of $X < 1$ will have large concentration of sulphur vacancies (V_S) [11]. These vacancies creates shallow donor levels (electron traps) below the conduction band (CB) edge whereas the dopant ions such as Al^{3+}, substituted for Zn^{2+} (Al_{Zn}), also creates donor levels but deeper in position than the VS [12]. Further, the Cu^{+} ions, substitutionally situated at the Zn^{2+}

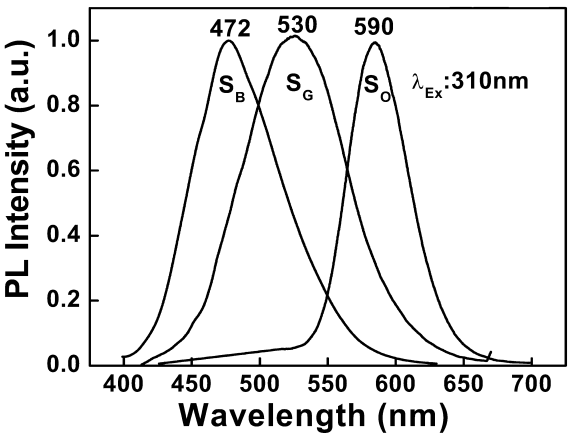

Fig. 2. PL spectra showing blue, green and orange–red emission from PVP capped ZnS: 0.13% Cu^{+} (S_B), ZnS: 0.13% Cu^{+}; 0.1% Al^{3+} (S_G), and ZnS: 0.2% Mn^{2+} (S_O) nanoparticles.

site (Cu_{Zn}), form acceptor levels (hole traps) above the valance band (VB) [13]. In the present study, the blue emission at 462 nm from the sample S_B, prepared under $X < 1$ condition, is attributed to the electronic transition involving both V_S and Cu_{Zn} ($V_S \rightarrow Cu_{Zn}$). The introduction of Al^{3+} together with Cu^{+} under stoichiometric condition of $X > 1$ (S_G) resulted in green emission due to dominant $Al_{Zn} \rightarrow Cu_{Zn}$ transition. Further, the orange emission at 590 nm from S_O nanocrystals is ascribed to $^4T_1 \rightarrow {}^6A_1$ transition in the *d*-orbital electronic states (d–d transition) of Mn^{2+} ions substitutionally situated at Zn^{2+} sites [14].

The photoluminescence excitation (PLE) spectrum recorded for multiple emissions from bulk ZnS phosphors, P-ZnS and PVP-ZnS nanocrystals are shown in Fig. 3. In case of bulk ZnS, the PLE band shows a sharp peak maximum at 340 nm (3.67 eV) indicative of the energy transfer from the band-to-band excitation of microcrystalline ZnS host lattice having well defined s–p band states. In case of pyridine capped nanocrystals, the PLE spectrum shows a narrow, symmetric band with peak maximum at 310 nm (4.0 eV). The blue shift in the PLE of nanocrystals is attributed to quantum confinement effects [15].

We now examine the PLE spectra of PVP capped nanocrystals. Curves (c)–(h) refer to the excitation spectra of samples prepared by increasing the PVP concentration from 0–1.2 wt%. Interestingly, it can be seen that the excitation spectrum is significantly modified due to the appearance of a set of new high-energy excitation bands. With increasing PVP concentration, the intensity of these additional bands increases resulting into remarkable broadening of the PLE spectrum. Similar modifications have also been observed with change in the concentration or type of the solvent medium (water, DMF or acetone). Gaussian curve fitting is applied to de-convolute the multiple bands that constitute the envelope spectrum. The highly broadened PLE of 1.0% PVP-ZnS sample has been deconvoluted into five different bands (Fig. 3(i)) with peak maximum at 235, 253, 260, 275 and 310 nm. The relative intensities of each of these bands vary with change in the concentration of PVP. The band with maximum around 310 nm can be attributed to the band-to-band excitation of the nanocrystalline ZnS host whereas the high energy bands from 235–275 nm are not expected from the ZnS host, as these maxima were not seen either in case of bulk ZnS or P-ZnS. We have estimated the integrated PLE intensity contributed by the ZnS host (area under 310 nm band) and the high energy bands from 235 to 275 nm and found that the PLE intensity due to the high energy bands scale-up with increase in the PVP concentration as shown in Fig. 4 (inset-i). Further, the excitation of doped PVP-ZnS samples using any radiation between 235 and 275 nm gives rise to strong dopant related emission as shown in case of PVP-ZnS:Mn (Fig. 4(c)). However, it can be seen that the Mn^{2+} related orange emission (590 nm) has been accompanied by a weak side band at 430 nm. This emission band was absent under 310 nm excitation, i.e. band-to-band excitation of ZnS host, indicating its different origin from that of the ZnS. With increase in the concentration of Mn^{2+}, the intensities of 590 nm emission and corresponding PLE increases (Fig. 3 inset-ii), whereas the intensity of blue emission band at 430 nm decreases.

Band-to-band excitation maximum of nanocrystalline semiconductor can be blue shifted or broadened due to (i) quantum confinement effects or (ii) high polydispersity [15]. However, in the frame of well accepted effective mass

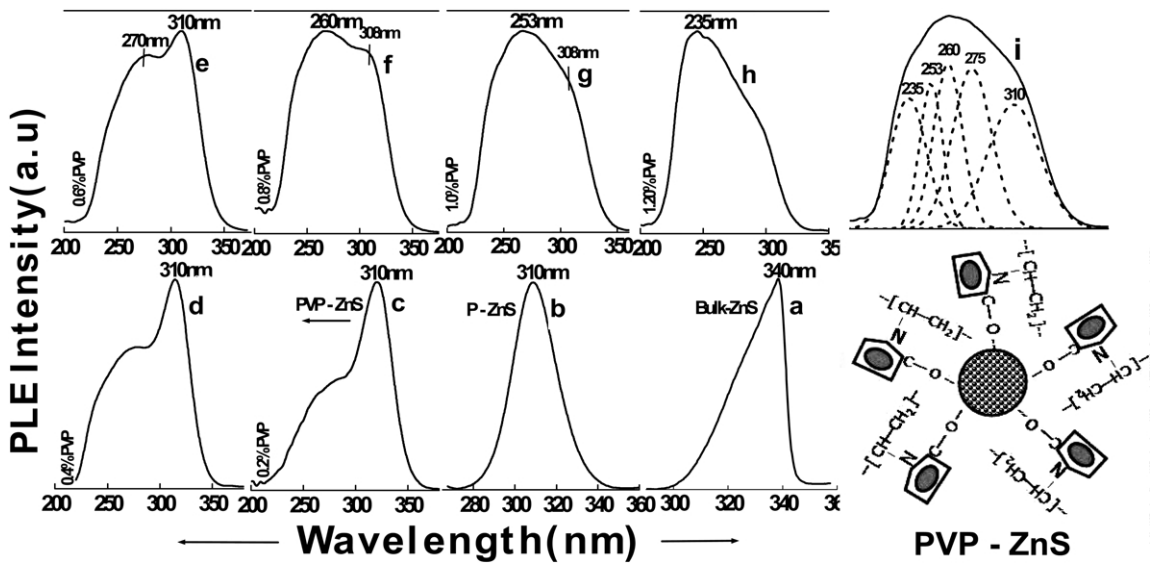

Fig. 3. PLE spectra corresponding to dopant related emissions from ZnS phosphors (a) Bulk ZnS, (b) P-ZnS nanoparticles, (c–h) PVP-ZnS nanoparticles with increase in PVP concentration. (i) Deconvoluted PLE of 1% PVP-ZnS showing the presence of multiple excitation bands in PVP capped nanoparticles. Schematic: Illustration of PVP capped ZnS nanoparticles.

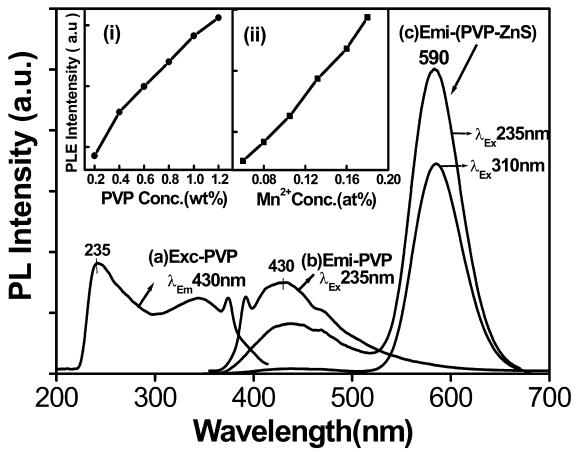

Fig. 4. Luminescence characteristics of aqueous PVP solution and PVP-ZnS:Mn nanoparticles. (a) PLE spectrum recorded for 430 nm emission from PVP solution, (b) PL emission from PVP solution and (c) PL from PVP-ZnS:Mn under 235 and 310 nm excitations. Inset: Increase in the integrated PLE intensity with (i) PVP concentration and (ii) Mn^{2+} concentration.

approximation theory, the maximum size dependant blue shift in E_g that can occur for ~4 nm sized ZnS particles of zinc-blende structure is 0.6 eV [16]. Therefore, the larger shift in ΔE_g by ~1.23 eV (i.e., from 3.67 to 4.9 eV) observed in the case of PVP-ZnS cannot be attributed to the quantum size effects. Further, the TEM studies show low polydispersity for PVP-ZnS particles as compared to P-ZnS. Moreover, we have observed broadening in the PLE due to changes in the concentration or type of the solvent used to disperse a given ensemble of nanoparticles (i.e., fixed polydispersity). Therefore, the broadening in the PLE due to PVP capping cannot be also accounted by polydispersity in particle size. In this context, we believe that, the high energy bands in the PLE of PVP-ZnS nanoparticles are originated from the energy levels other than that host ZnS, probably from the surface adsorbed PVP molecules.

We now discuss the PL spectra of 1% PVP aqueous solution, shown in Fig. 4(a) and (b). It is interesting to see that the PVP is weakly emissive with peak maximum at 430 nm and the corresponding excitation spectrum has multiple peak maxima at 235, 260, 340 and 374 nm. These excitation bands are attributed to the electronic transitions in PVP molecular orbitals (delocalized) involving the C=O groups by way of S_0–S_1 (π–π^*), S_0–S_1 (n-π^*) and S_0–T_1 (n-π^*) transitions [17]. The blue emission band at 430 nm is attributed to the radiative relaxation of electrons from LUMO to HOMO levels in PVP.

In view of the above results, it is reasonable to state that: (i) the high energy bands observed in the PLE spectrum of PVP-ZnS nanocrystals are contributed by the surface adsorbed PVP molecules, (ii) efficient energy transfer takes place from the molecular orbital levels of surface adsorbed PVP to luminescent centers in doped ZnS, and (iii) energy transfer efficiency from PVP to luminescent centers increases with the concentration of both PVP as well as dopant ions.

Pyrrolidone moiety in PVP has both N as well as C=O groups. Studies on zinc-pyrrolidone-carboxylate complex systems [18] show that the oxygen in carboxylates makes coordinate bonding with the Zn atoms whereas the lone pair electron on nitrogen in pyrrolidone is conjugated with the adjacent carbonyl group. In PVP-ZnS samples, we expect a similar bonding at the surface of nanoparticles wherein C=O groups coordinate with the metal ions to form –C=O → Zn^{2+} (Mn^{2+}, Cu^{+}, Al^{3+}) bonds which can give rise to overlapping of molecular orbitals of PVP with atomic orbitals of metal ions, particularly located at the surface regions. These interactions can cause both (i) alteration of the tautomeric form of surface adsorbed organic molecules due to change in effective charge on N and C=O and (ii) transfer the excited state energy from the molecular orbital of PVP to ZnS nanocrystals. We believe that the excitation peaks at 235, 253 and 260 nm arise from enol-tautomer of pyrrolidone whereas 275 and 290 nm are from the keto form of pyrrolidone moiety. Electrostatic interaction of the adsorbed molecules, leading to hydrogen bonding with C=O as well as N groups, will change the charge distribution in the molecules, resulting in enhanced electronic delocalization which changes with the concentration, nature of solvent as well as the intermolecular interactions in the chemisorbed layers. This together with the vibrational relaxations account for the broad, multiple maxima in the excitation spectra of the adsorbed PVP molecules.

Fig. 5 shows energy transfer scheme depicting different electronic transitions leading to emission in Mn^{2+} doped bulk ZnS, P-ZnS and PVP-ZnS. For bulk as well as P-ZnS, the band-to-band transition energy is transferred on to Mn^{2+} centers causing the d–d excitation wherein the $^4T_1 \rightarrow {}^6A_1$ radiative relaxation gives rise to the orange emission at 590 nm. In the case of PVP capped ZnS:Mn, in addition to the above excitation mechanism, chemisorbed capping molecules also transfers energy directly to the Mn^{2+} centers, particularly at higher concentrations of the polymer. Thus, two different excitation paths prevail for the luminescence in PVP-ZnS:Mn nanocomposites. The position of the energy states of adsorbed molecules is labile relative to the band edge energy values of the semiconductor. However, the multiplicity in the molecular energy states of the organic adsorbate enhances the probability of energy transfer and increase the emission efficiency.

4. Summary

In summary, enhanced photoluminescence has been observed from the doped ZnS nanocrystals due to efficient energy transfer from the surface adsorbed PVP molecules to dopant centers in nanocrystals. The energy transfer

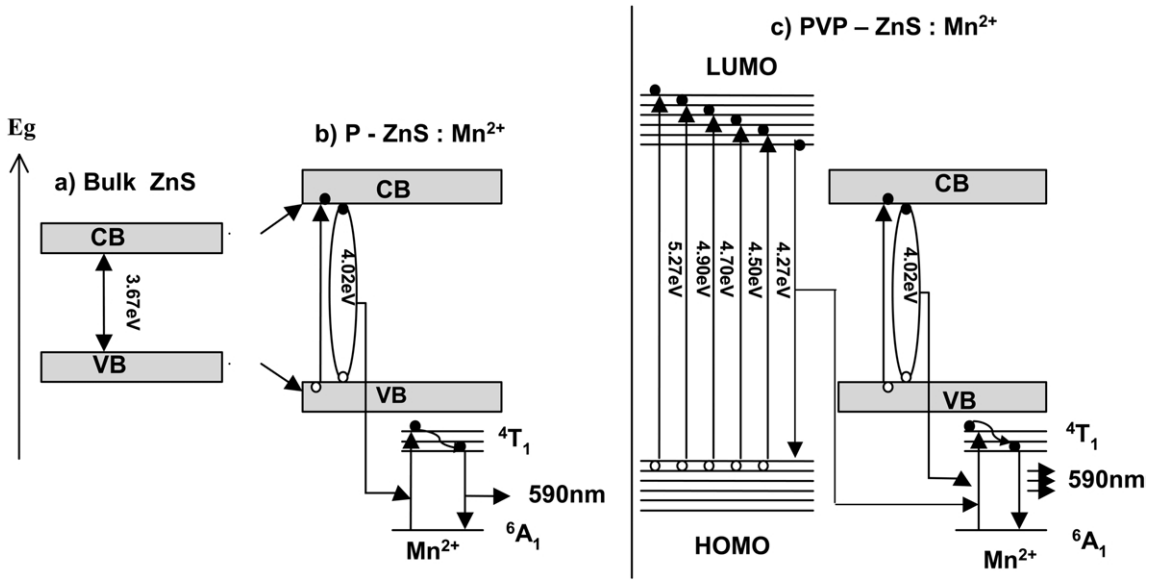

Fig. 5. Schematic illustration of various electronic transitions and energy transfer process involved in (a) Bulk ZnS:Mn, (b) P-ZnS:Mn, and (c) PVP-ZnS:Mn.

efficiency has been found to increase with the concentration of PVP or dopants. This study brings out a new sensitizer (energy donor)—activator (energy acceptor) type relation between the polymeric capping agent and luminescent semiconducting nanoparticles. Because of the easy dispersion of the PVP-ZnS composites, highly photoluminescent polymer nanocomposites can be prepared by embedding these particles in transparent plastic media. Further, compositing with semiconducting polymers, organic-quantum dot hybrid electroluminescent displays can also be realized from these nanoparticles.

Acknowledgements

The authors thank Mr R.K. Syal, Director, Defence Laboratory for his support to this work. The authors also thank Prof. G.N. Subbanna and Mr. C. Sudhakar of MRC, IISc, Bangalore for their help in recording the XRD patterns and TEM images of the samples.

References

[1] M.L. Steigerwald, L.E. Brus, Acc. Chem. Res. 23 (1990) 283.
[2] A.P. Alivisatos, Science 271 (1996) 933.
[3] M. Nirmal, B.O. Dabbousi, M.G. Bawendi, J.K. Trautman, T.D. Harris, L.E. Brus, Nature 383 (1996) 802.
[4] C.B. Murray, D.J. Norris, M.G. Bawendi, J. Am. Chem. Soc. 115 (1993) 8706.
[5] T. Igarashi, T. Isobe, M. Senna, Phys. Rev. B 56 (1997) 6444.
[6] R.N. Bhargava, D. Gallagher, Phys. Rev. Lett. 72 (1994) 416.
[7] C.J. Murphy, Appl. Spectrosc. 56 (2002) 16A.
[8] S. Coe, K.W. Woo, M.G. Bawendi, V. Bulovic, Nature 420 (2003) 800.
[9] K. Manzoor, S.R. Vadera, N. Kumar, T.R.N. Kutty, Mater. Chem. Phys. (2003) in press.
[10] S.B. Qudri, E.F. Skelton, D. Hsu, A.D. Dinsmore, J. Yang, H.F. Gray, B.R. Ratna, Phys. Rev. B 60 (1999) 9191.
[11] J.F. Suyver, S.F. Wuister, J.J. Kelly, A. Meijerink, Nano Lett. 1 (2000) 429.
[12] S. Shinoya, W.M. Yen, Phosphor Handbook, CRC Press, Washington, 1999.
[13] A.S. Marfunin, Spectroscopy, Luminescence and Radiation Centers in Minerals, Springer, New York, 1979.
[14] K. Sooklal, B.S. Cullum, S.M. Angel, C.J. Murphy, J. Phys. Chem. 100 (1996) 4551.
[15] L. Brus, J. Chem. Phys. 80 (1984) 4403.
[16] R. Rossetti, R. Hull, J.M. Gibson, L.E. Brus, J. Chem. Phys. 82 (1985) 552.
[17] M. Klessinfer, J. Michl, Excited States and Photochemistry of Organic Molecules, VCH, Weinheim, 1995.
[18] G.D. Parfitt, A.V. Patsis, Organic Coatings: Science and Technology, Marcel Dekker Inc, New York, 1984.